

MERGETUNE: CONTINUED FINE-TUNING OF VISION-LANGUAGE MODELS

Wenqing Wang^{1*}, Da Li^{2,3*}, Xiatian Zhu^{1†}, Josef Kittler^{1†}

¹ University of Surrey

² Samsung AI Centre Cambridge

³ Queen Mary University of London

ABSTRACT

Fine-tuning vision-language models (VLMs) such as CLIP often leads to catastrophic forgetting of pretrained knowledge. Prior work primarily aims to mitigate forgetting during adaptation; however, forgetting often remains inevitable during this process. We introduce a novel paradigm, *continued fine-tuning (CFT)*, which seeks to recover pretrained knowledge after a zero-shot model has already been adapted. We propose a simple, model-agnostic CFT strategy (named MERGETUNE) guided by linear mode connectivity (LMC), which can be applied post hoc to existing fine-tuned models without requiring architectural changes. Given a fine-tuned model, we continue fine-tuning its trainable parameters (e.g., soft prompts or linear heads) to search for a continued model which has two low-loss paths to the zero-shot (e.g., CLIP) and the fine-tuned (e.g., CoOp) solutions. By exploiting the geometry of the loss landscape, the continued model implicitly merges the two solutions, restoring pretrained knowledge lost in the fine-tuned counterpart. A challenge is that the vanilla LMC constraint requires data replay from the pretraining task. We approximate this constraint for the zero-shot model via a second-order surrogate, eliminating the need for large-scale data replay. Experiments show that MERGETUNE improves the harmonic mean of CoOp by +5.6% on base-novel generalisation without adding parameters. On robust fine-tuning evaluations, the LMC-merged model from MERGETUNE surpasses ensemble baselines with lower inference cost, achieving further gains and state-of-the-art results when ensembled with the zero-shot model. Our code is available at <https://github.com/Surrey-UP-Lab/MERGETUNE>.

1 INTRODUCTION

Foundational vision-language models (VLMs) such as CLIP (Radford et al., 2021) have achieved strong zero-shot generalisation by pretraining on web-scale image-text pairs. To further adapt these models for downstream tasks, fine-tuning is often necessary. However, a well-known drawback of fine-tuning VLMs is catastrophic forgetting of pretrained knowledge, which weakens generalisation.

A range of fine-tuning strategies have been proposed to address this issue, though under different evaluation protocols. Parameter-efficient fine-tuning (PEFT) methods update only lightweight modules such as prompts (Zhou et al., 2022b;a; Yao et al., 2023; Li et al., 2025) or adapters (Yang et al., 2024; Khattak et al., 2023), achieving strong adaptation with relatively a smaller amount of trainable parameters. These approaches are primarily evaluated under few-shot settings, focusing on base-to-novel generalisation and, to a lesser extent, cross-domain and cross-dataset generalisation. In parallel, robust fine-tuning approaches (Wortsman et al., 2022b; Zhu et al., 2024) combine pretrained and finetuned models through ensembling, either in weight space (Wortsman et al., 2022a; Huang et al., 2024) or prediction space (Lakshminarayanan et al., 2017). Unlike PEFT methods, robust fine-tuning methods are typically evaluated in many-shot settings, aligning with standard domain generalisation benchmarks (Zhou et al., 2023) while enforcing great in-distribution performance.

*Equal contribution

†Joint last authorship

While PEFT methods mitigate forgetting by restricting updates to lightweight modules, they not only rely on increasingly complex modules (Yang et al., 2024) to balance adaptation with generalisation, but also still preserve pretrained knowledge incompletely. For example, as shown in Figure 1, no single prior PEFT method consistently outperforms CLIP across all 11 evaluation datasets without leveraging external knowledge (Yao et al., 2024). Similarly, ensembling can ease forgetting in the robust fine-tuning, but they often fail to fully reconcile pretrained knowledge with downstream adaptation (Zhu et al., 2024) and yield unstable performance (as shown in Table 4).

In this paper, we explore how to recover forgotten knowledge after fine-tuning is completed, which resembles the purpose of model ensembling methods in the robust fine-tuning (Wortsman et al., 2022b; Zhu et al., 2024). However, unlike ensembling, we take it as a post hoc direction to the VLM adaptation techniques through *continued fine-tuning*.

We take inspiration from recent advanced weight-space ensembling – model merging (Yadav et al., 2023; Huang et al., 2024), which demonstrates that different models can be combined to integrate complementary knowledge. Building on these insights, we propose to merge a finetuned VLM with its zero-shot counterpart to restore lost knowledge and enhance performance. However, existing model merging methods are often ineffective in this context, where the zero-shot and finetuned models could lie far apart in weight space. This weight-space gap could break the mode connectivity (Garipov et al., 2018) required for model merging to be effective and may explain the unstable performance commonly observed in weight averaging approaches (Wortsman et al., 2022a; Zhu et al., 2024). To overcome this, we propose a learning-based merging method that leverages linear mode connectivity (LMC) (Garipov et al., 2018) as an objective to integrate knowledge from both zero-shot and finetuned VLMs through continued fine-tuning.

Our model-agnostic MERGETUNE applies post hoc to already finetuned VLMs without requiring architectural changes. We can continue updating its trainable parameters (e.g., soft prompts, adapters, or linear heads) accordingly to search for weights that are connected to the zero-shot and the finetuned ones with two low-loss paths. The continued fine-tuning by searching these geometrically linear paths allows the continued model to effectively integrate pretrained knowledge into the finetuned model. However, the vanilla LMC constraint requires replaying the data used for training the zero-shot model (Mirzadeh et al., 2021), which is problematic. For example, the web-scale corpus used for pretraining CLIP is publicly inaccessible (Radford et al., 2021). And even accessible for replay, it is computationally prohibitive. We thus introduce a second-order surrogate that approximates the constraint for the zero-shot model, eliminating the need for large-scale data replay.

We apply MERGETUNE to multiple PEFT and robust fine-tuning methods. Experiments demonstrate that MERGETUNE consistently improves accuracies on the benchmarks for which these models were trained. On base-to-novel generalisation, MERGETUNE improves the harmonic mean of CoOp (Zhou et al., 2022b) by +5.6% without adding parameters. On robust fine-tuning tasks, the LMC-merged model from MERGETUNE achieves stronger out-of-distribution (OOD) generalisation than ensemble-based baselines, while maintaining comparable in-distribution (ID) accuracy. It also reduces inference cost and consistently outperforms CLIP across all evaluated cases. Moreover, simple ensembling with the zero-shot model brings further gains, setting new state-of-the-art results.

We summarise our contributions as follows: 1) While existing VLM methods seek to mitigate knowledge forgetting during downstream fine-tuning, we find that forgetting remains often unavoidable. In response, we propose *continued fine-tuning* — a new paradigm to existing methods — to restore

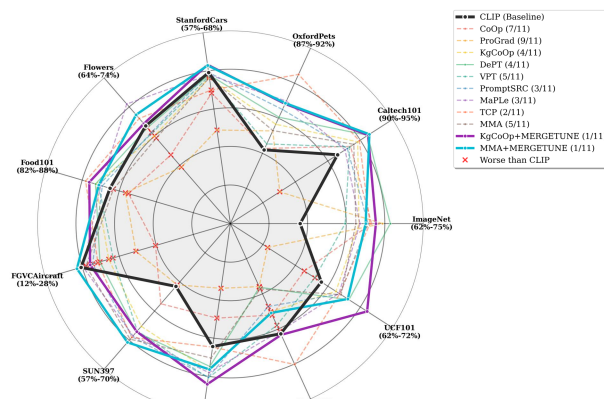


Figure 1: Cross-dataset generalisation shows no single PEFT method consistently outperforms CLIP across all 11 datasets, implying incomplete preservation of pretrained knowledge. Numbers in brackets ($X/11$) indicate X times a method underperforms CLIP.

forgotten knowledge after the model has been adapted. 2) Inspired by model merging (Section 3), which integrates complementary knowledge across models, we introduce a learning-based merging method MERGETUNE guided by linear mode connectivity (Section 4). 3) MERGETUNE is model-agnostic and can be applied post hoc to any fine-tuned VLM without architectural changes. Extensive experiments demonstrate its effectiveness in restoring pretrained knowledge to enhance the fine-tuned model (Section 5).

2 RELATED WORK

VLM fine-tuning. Few-shot parameter-efficient fine-tuning (PEFT) has become a common strategy for adapting vision-language models (VLMs), as it reduces computational costs while mitigating catastrophic forgetting. Prompt learning methods, such as CoOp (Zhou et al., 2022b) and CoCoOp (Zhou et al., 2022a), optimise continuous prompts (task-specific or image-conditioned) instead of fixed templates, with extensions including prompt distributions (Lu et al., 2022) and attribute-guided prompts (Li et al., 2025). Adapter-based methods insert lightweight trainable modules, either uni-modal (Clip-Adapter (Gao et al., 2024), Tip-Adapter (Zhang et al., 2022)) or multi-modal (Yang et al., 2024; Jiang et al., 2025; Zang et al., 2022). Most of these existing methods focus on the few-shot learning evaluation of base-to-novel generalisation, with limited attention to cross-domain and cross-dataset generalisation.

Another line of work focuses on many-shot robust fine-tuning (Zhou et al., 2023), aiming to boost in-distribution accuracy without compromising out-of-distribution generalisation (Kumar et al., 2022; Wortsman et al., 2022b; Zhu et al., 2024). One common practice is weight ensembling after the model is fine-tuned, which blends zero-shot and fine-tuned model parameters to preserve both task-specific and general capabilities. Wortsman et al. (2022b) demonstrated that simple linear interpolation between zero-shot and fine-tuned weights can improve both ID and OOD performance. More sophisticated ensemble methods have emerged, such as VRF (Zhu et al., 2024), which conditionally combines models based on a "zero-shot failure" set, and R-Adapter (Kim et al., 2024), which integrates self-ensembling with lightweight adaptation. However, these complex ensembling procedures add inference overhead.

Model merging. Model merging demonstrates that different models can be effectively combined to integrate complementary knowledge, grounded in the discovery of mode connectivity (Garipov et al., 2018). Early work showed that independently trained solutions can be linked by low-loss paths in weight space (Garipov et al., 2018; Draxler et al., 2018). Building on these insights, practical methods emerged: model soups combine multiple fine-tuned weights (Wortsman et al., 2022a), task arithmetic edits task vectors (Ilharco et al., 2023), and approaches like TIES-Merging (Yadav et al., 2023) and DARE (Yu et al., 2024) address interference during model merging.

Instead of merely mitigating forgetting during downstream fine-tuning, our goal is to restore the pretrained knowledge lost after the zero-shot model has been adapted. To this end, we introduce a *continued fine-tuning* strategy MERGETUNE that learns to merge the zero-shot and adapted models.

3 PRELIMINARIES

We begin by introducing model merging and mode connectivity, which underpin our approach.

Model merging and mode connectivity. When two models are trained on the same task with the loss $\mathcal{L}(\cdot)$ but differ in initialisation or training trajectory, they converge to different solutions \hat{w}_1, \hat{w}_2 that both achieve low loss. Often, one can merge them through weight averaging,

$$w = \gamma(\alpha) = (1 - \alpha)\hat{w}_1 + \alpha\hat{w}_2, \quad \alpha \in [0, 1]. \quad (1)$$

This linear interpolation can sometimes yield a model with performance comparable to its endpoints \hat{w}_1 and \hat{w}_2 (Izmailov et al., 2018) or yield an interesting observation (Garipov et al., 2018) as follows

$$\mathcal{L}(\gamma(\alpha)) \approx 0, \quad (2)$$

i.e. during the interpolation, the computed loss of the resulting model is consistently close to 0.

The effectiveness of model merging and the root of the observation in Eq. 1 can be explained by the phenomenon of mode connectivity (Garipov et al., 2018; Draxler et al., 2018), i.e. linear mode

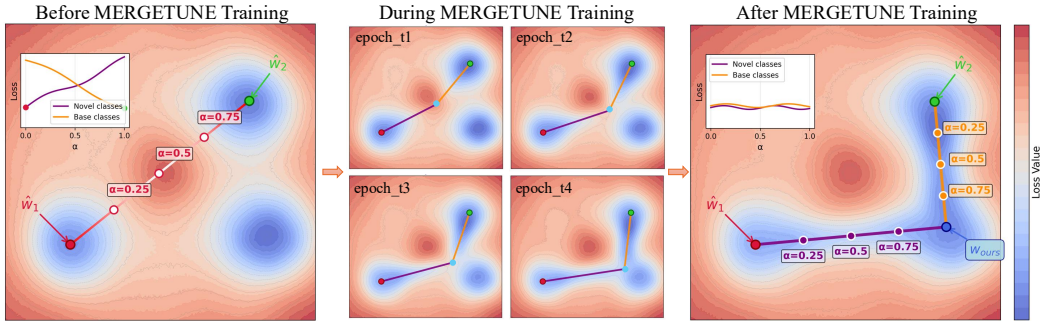


Figure 2: The proposed MERGETUNE (conceptual illustration). (Left) Before MERGETUNE Training: The zero-shot model \hat{w}_1 and fine-tuned \hat{w}_2 exist in separate minima with no low-loss connectivity. Linear interpolation between them (shown in the inset) reveals high barriers and induces a performance trade-off on base and novel classes. (Middle) During training, w is searched to mode connected to both \hat{w}_1 and \hat{w}_2 , gradually integrating both models. (Right) After MERGETUNE Training: Our continued model w_{ours} merging two endpoints will be used for inference of both tasks \hat{w}_1 and \hat{w}_2 where trained. The two distinct low-loss paths, $\hat{w}_1 \rightarrow w_{ours}$ and $\hat{w}_2 \rightarrow w_{ours}$, show smooth interpolation curves (inset) indicating stable performance.

here. Empirical studies have shown that seemingly distinct optima discovered by independent training runs can be linked by continuous low-loss paths in parameter space. This indicates that neural network solutions are not totally isolated minima but could lie in connected valleys of the loss landscape. Mode connectivity thus provides a theoretical basis for why interpolation between models can preserve low loss.

Merging models of different tasks. Beyond the same-task setting above, model merging can be extended to integrate knowledge from different but related tasks, e.g., combining a model with another trained for different tasks (Mirzadeh et al., 2021; Yadav et al., 2023; Yu et al., 2024). In this case, the goal is to find a merged solution w that preserves performance on both tasks. Formally, given two models \hat{w}_1 and \hat{w}_2 trained with task losses \mathcal{L}_1 and \mathcal{L}_2 , one can seek a new model w whose interpolation paths to \hat{w}_1 and \hat{w}_2

$$\gamma_1(\alpha) = \hat{w}_1 + \alpha(w - \hat{w}_1), \quad \gamma_2(\alpha) = \hat{w}_2 + \alpha(w - \hat{w}_2), \quad \alpha \in [0, 1], \quad (3)$$

satisfy

$$\mathcal{L}_1(\gamma_1(\alpha)) \approx 0, \quad \mathcal{L}_2(\gamma_2(\alpha)) \approx 0. \quad (4)$$

That is, throughout the interpolation, model w maintains two smooth, low-loss connections to both endpoints, ensuring that knowledge from both tasks is preserved in the single w (Mirzadeh et al., 2021; Yadav et al., 2023; Yu et al., 2024).

From this perspective, model merging can be viewed as finding a solution that lies on low-loss paths connecting multiple checkpoints. This geometric view unifies heuristic averaging methods, such as training-free approaches TIES (Yadav et al., 2023) and DARE (Yu et al., 2024), with regularisation-based methods (Mirzadeh et al., 2021). Enforcing mode connectivity ensures that the merged model integrates the endpoints, preserving knowledge from both. However, training-free methods (Yadav et al., 2023; Yu et al., 2024) lack explicit enforcement of mode connectivity, and may therefore struggle to integrate models effectively.

4 MERGETUNE: CONTINUED FINETUNING OF VLMS VIA MODE-CONNECTIVITY GUIDANCE

We now introduce our continued fine-tuning (CFT) objective, which enforces *linear mode connectivity* between the continued model and both the zero-shot and fine-tuned solutions. This ensures that the final model preserves pretrained knowledge while retaining downstream adaptation.

Linear mode connectivity as an objective. The effectiveness of model merging is grounded in the phenomenon of linear mode connectivity. We employ it directly as a learning principle, as inspired by Eq. 3 and Eq. 4. Our hypothesis is that if a model can be linearly connected to another solution through a consistently low-loss path, it can inherit and preserve the knowledge of that solution.

Concretely, given a zero-shot checkpoint \hat{w}_1 (e.g., CLIP) and a downstream fine-tuned checkpoint \hat{w}_2 (e.g., CoOp), we seek a continued solution w that integrates both. We require w to remain linearly connected to both \hat{w}_1 and \hat{w}_2 via low-loss interpolations. This leads to the objective:

$$w = \arg \min_w \mathbb{E}_{\alpha \sim \mathcal{U}[0,1]} \left[\mathcal{L}_1(\hat{w}_1 + \alpha(w - \hat{w}_1)) + \mathcal{L}_2(\hat{w}_2 + \alpha(w - \hat{w}_2)) \right], \quad (5)$$

where \mathcal{L}_1 and \mathcal{L}_2 are the pretraining and downstream training losses for the zero-shot and fine-tuned models, and α is the interpolation coefficient uniformly sampled from $[0, 1]$. This formulation leverages linear mode connectivity as a learning objective to merge knowledge from two solutions. After training, w is used for inference. An illustration of our training process is shown in Figure 2.

Challenge. A direct implementation of Eq. 5 requires the computation of both \mathcal{L}_1 and \mathcal{L}_2 . However, \mathcal{L}_1 depends on the pretraining data (e.g., CLIP’s web-scale corpus), which is often inaccessible and computationally prohibitive to replay. Thus, we propose a second-order surrogate loss to approximate the computation of Task 1 loss term in a replay-free manner.

Second-order surrogate. We approximate the Task 1 interpolation term using a second-order Taylor expansion:

$$\mathcal{L}_1(\hat{w}_1 + \alpha(w - \hat{w}_1)) \approx \mathcal{L}_1(\hat{w}_1) + \alpha \nabla \mathcal{L}_1(\hat{w}_1)^\top (w - \hat{w}_1) + \frac{\alpha^2}{2} (w - \hat{w}_1)^\top H_1 (w - \hat{w}_1), \quad (6)$$

where $H_1 = \nabla^2 \mathcal{L}_1(\hat{w}_1)$ is the Hessian matrix.

We adopt two assumptions: (1) $\nabla \mathcal{L}_1(\hat{w}_1) \approx 0$, as \hat{w}_1 lies near a local optimum for Task 1. (2) $H_1 \approx \mu I$, assuming isotropic curvature for tractability following common practices. Under these assumptions, Eq. 6 simplifies to:

$$\mathcal{L}_1(\hat{w}_1 + \alpha(w - \hat{w}_1)) \approx \mathcal{L}_1(\hat{w}_1) + \frac{\mu \alpha^2}{2} \|w - \hat{w}_1\|^2. \quad (7)$$

$\mathcal{L}_1(\hat{w}_1)$ is a constant value, and $\frac{\mu \alpha^2}{2}$ can be represented by λ . The surrogate regulariser can be formulated as:

$$\mathcal{R}_{\text{Task1}} = \lambda \|w - \hat{w}_1\|^2. \quad (8)$$

Final replay-free objective. Combining the Task 1 surrogate with the Task 2 objectives leads to our final continued fine-tuning loss:

$$\mathcal{L}(w) = \mathcal{L}_2(w) + \lambda \|w - \hat{w}_1\|^2 + \beta \mathbb{E}_{\alpha \sim \mathcal{U}[0,1]} \mathcal{L}_2(\hat{w}_2 + \alpha(w - \hat{w}_2)). \quad (9)$$

This objective preserves pretrained knowledge through proximity to \hat{w}_1 , while enforcing low-loss connectivity to the downstream solution \hat{w}_2 . Empirically, we decoupled $\mathcal{L}_2(w)$, where $\alpha = 1$, from the expectation term. In this way, the LMC terms serve as a regulariser for training. Also, the expectation in the third term is computationally intractable. We thus approximate it by evaluating a small number of evenly spaced α values (e.g., five or ten), which yields promising results.

Application to CLIP fine-tuning methods. Our framework makes no limitation on which parameters are trainable, allowing it to be applied broadly. We optimise w under the same training configurations as the base method: In prompt-based methods such as CoOp and KgCoOp¹, $w = T(p)$ corresponds to the classifier weights derived from learnable prompts p and $T(\cdot)$ is the text encoder. In adapter-based methods such as MMA, $w = T(p; \theta)$ includes fixed prompts and trainable multimodal adapters θ . In many-shot regimes, w can represent the linear classification head (linear probing) or the entire model parameters (end-to-end fine-tuning). This flexibility allows our continued fine-tuning approach to act as a general post hoc enhancement, seamlessly integrating with diverse CLIP adaptation strategies.

5 EXPERIMENTS

We evaluate MERGETUNE across multiple benchmarks and protocols:

¹Also interesting to note, our MERGETUNE reduces to KgCoOp when $\beta=0$ for prompt tuning.

Table 1: Base-to-novel generalisation experiments on 11 datasets. Our method achieves consistent average performance improvement over different baselines. \dagger : Using large language model or teacher model’s knowledge.

Method	Average			ImageNet			Caltech101			OxfordPets		
	Base	Novel	HM	Base	Novel	HM	Base	Novel	HM	Base	Novel	HM
CLIP (ICML 21)	69.34	74.22	71.70	72.43	68.14	70.22	96.84	94.00	95.40	91.17	97.26	94.12
CoOp (IJCV 22)	82.69	63.22	71.66	76.47	67.88	71.92	98.00	89.81	93.73	93.67	95.29	94.47
KgCoOp (CVPR 22)	80.73	73.61	77.01	75.83	69.96	72.78	97.72	94.39	96.03	94.65	97.76	96.18
MaPLe (CVPR 23)	82.28	75.14	78.55	76.66	70.54	73.47	97.74	94.36	96.02	95.43	97.76	96.58
PromptSRC (ICCV 23)	84.26	76.10	79.97	77.60	70.73	74.01	98.10	94.03	96.02	95.33	97.30	96.30
MMA (CVPR 24)	83.20	76.80	79.87	77.31	71.00	74.02	98.40	94.00	96.15	95.40	98.07	96.72
CoPrompt \dagger (ICLR 24)	84.00	77.23	80.48	77.67	71.27	74.33	98.27	94.90	96.55	95.67	98.10	96.87
PromptKD \dagger (CVPR 24)	86.96	80.73	83.73	80.83	74.66	77.62	98.91	96.65	97.77	96.30	98.01	97.15
CoOp + ATPrompt \dagger (ICCV 25)	82.68	68.04	74.65 (4.29)	76.27	70.60	73.33	97.95	93.63	95.74	94.77	96.59	95.67
PromptKD + ATPrompt \dagger (ICCV 25)	87.05	81.82	84.35 (4.62)	80.90	74.83	77.75	98.90	96.52	97.70	96.92	98.27	97.59
CoOp + TIES (NeurIPS 23)	66.95	65.71	66.32 (-5.33)	70.09	61.65	65.60	93.63	91.34	92.50	90.12	95.13	92.56
CoOp + DARE (ICML 24)	75.91	65.97	70.59 (-1.07)	74.25	64.32	68.93	96.36	91.12	93.67	93.41	96.33	94.84
CoOp + MERGETUNE	80.82	73.97	77.24 (4.58)	75.96	69.91	72.81	97.91	94.65	96.25	95.09	97.75	96.40
KgCoOp + TIES (NeurIPS 23)	73.03	72.09	72.56 (-4.45)	74.06	68.06	70.93	97.27	94.43	95.83	93.99	96.51	95.23
KgCoOp + DARE (ICML 24)	78.15	72.41	75.17 (-1.84)	75.10	68.73	71.78	97.53	94.47	95.97	92.22	97.37	94.73
KgCoOp + MERGETUNE	81.85	74.46	77.98 (4.07)	76.49	69.35	72.75	97.87	94.91	96.37	95.32	97.76	96.53
MMA + TIES (NeurIPS 23)	70.39	68.46	69.41 (-10.46)	73.16	66.48	69.66	95.36	92.23	93.77	91.24	93.11	92.17
MMA + DARE (ICML 24)	74.25	69.52	71.81 (-8.06)	74.17	66.76	70.27	94.95	92.49	93.70	90.52	95.53	92.96
MMA + MERGETUNE	84.27	76.94	80.44 (4.57)	77.68	70.65	74.00	98.32	94.65	96.45	95.75	98.10	96.91
PromptKD \dagger + TIES (NeurIPS 23)	82.03	77.16	79.52 (-4.21)	76.12	69.32	72.56	97.61	94.9	96.24	95.23	96.13	95.68
PromptKD \dagger + DARE (ICML 24)	84.76	79.65	82.13 (-1.6)	78.29	72.54	75.31	98.12	96.19	97.15	95.56	98.00	96.76
PromptKD \dagger + MERGETUNE	87.23	81.17	84.09 (4.36)	80.89	74.88	77.77	98.93	96.64	97.77	96.63	98.34	97.48
Method	StanfordCars			Flowers102			Food101			FGVCAircraft		
	Base	Novel	HM	Base	Novel	HM	Base	Novel	HM	Base	Novel	HM
CLIP (ICML 21)	63.37	74.89	68.65	72.08	77.80	74.83	90.10	91.22	90.66	27.19	36.29	31.09
CoOp (IJCV 22)	78.12	60.40	68.13	97.60	59.67	74.06	88.33	82.26	85.19	40.44	22.30	28.75
KgCoOp (CVPR 22)	71.76	75.04	73.36	95.00	74.73	83.65	90.50	91.70	91.10	36.21	33.55	34.83
MaPLe (CVPR 23)	72.94	74.00	73.47	95.92	72.46	82.56	90.71	92.05	91.38	37.44	35.61	36.50
PromptSRC (ICCV 23)	78.27	74.97	76.58	98.07	76.50	85.95	90.67	91.53	91.10	42.73	37.87	40.15
MMA (CVPR 24)	78.50	73.10	75.70	97.77	75.93	85.48	90.13	91.30	90.71	40.57	36.33	38.33
CoPrompt \dagger (ICLR 24)	76.97	74.40	75.66	97.27	76.60	85.71	90.73	92.07	91.40	40.20	39.33	39.76
PromptKD \dagger (CVPR 24)	82.80	83.37	83.13	99.42	82.62	90.24	92.43	93.68	93.05	49.12	41.81	45.17
CoOp + ATPrompt \dagger (ICCV 25)	77.43	66.55	71.58	97.44	67.52	79.77	88.74	87.44	88.09	40.38	27.22	32.52
PromptKD + ATPrompt \dagger (ICCV 25)	82.51	84.03	83.26	99.15	82.03	89.78	92.48	93.86	93.22	49.63	42.35	45.70
CoOp + TIES (NeurIPS 23)	57.94	63.42	60.56	73.60	65.41	69.27	88.42	87.64	88.02	30.29	28.83	29.54
CoOp + DARE (ICML 24)	67.82	61.62	64.57	90.88	63.73	74.92	87.78	87.22	87.50	34.41	28.25	31.03
CoOp + MERGETUNE	71.94	75.12	73.49	95.32	74.30	83.51	90.56	91.75	91.15	36.17	34.35	35.24
KgCoOp + TIES (NeurIPS 23)	65.79	74.17	69.73	74.26	72.53	73.39	90.25	91.58	90.91	30.81	28.97	29.86
KgCoOp + DARE (ICML 24)	67.84	73.02	70.33	87.02	72.88	79.33	90.44	91.60	91.02	33.49	30.37	31.85
KgCoOp + MERGETUNE	73.21	75.14	74.17	96.49	74.68	84.20	90.51	91.83	91.17	37.09	35.11	36.07
MMA + TIES (NeurIPS 23)	60.72	70.12	65.08	73.46	70.74	72.07	88.79	89.83	89.31	29.27	28.06	28.65
MMA + DARE (ICML 24)	64.82	71.52	68.01	77.15	70.95	73.92	89.85	87.61	88.72	30.35	28.23	29.25
MMA + MERGETUNE	81.24	72.30	76.51	98.04	76.33	85.83	90.77	91.57	91.17	42.86	36.01	39.14
PromptKD \dagger + TIES (NeurIPS 23)	75.13	76.99	76.05	94.53	79.22	86.20	90.96	92.10	91.53	43.68	38.75	41.07
PromptKD \dagger + DARE (ICML 24)	80.13	81.95	81.03	97.73	80.93	88.54	91.57	93.28	92.42	46.96	40.79	43.66
PromptKD \dagger + MERGETUNE	82.98	83.90	83.44	99.30	82.67	90.23	92.45	93.91	93.17	49.82	42.31	45.76
Method	SUN397			DTD			EuroSAT			UCF101		
	Base	Novel	HM	Base	Novel	HM	Base	Novel	HM	Base	Novel	HM
CLIP (ICML 21)	69.36	75.35	72.23	53.24	59.90	56.37	56.48	64.05	60.03	70.53	77.50	73.85
CoOp (IJCV 22)	80.60	65.89	72.51	79.44	41.18	54.24	92.19	54.74	68.69	84.69	56.05	67.46
CoCoOp (CVPR 22)	79.74	76.86	78.27	77.01	56.00	64.85	87.49	60.04	71.21	82.33	73.45	77.64
KgCoOp (CVPR 22)	80.29	76.53	78.36	77.55	54.99	64.35	85.64	64.34	73.48	82.89	76.67	79.66
MaPLe (CVPR 23)	80.82	78.70	79.75	80.36	59.18	68.16	94.07	73.23	82.35	83.00	78.66	80.77
PromptSRC (ICCV 23)	82.67	78.47	80.52	83.37	62.97	71.75	92.90	73.90	82.32	87.10	78.80	82.74
MMA (CVPR 24)	82.27	78.57	80.38	83.20	65.63	73.38	85.46	82.34	83.87	86.23	80.03	82.20
CoPrompt \dagger (ICLR 24)	82.63	80.03	81.30	83.13	64.73	72.79	94.60	78.57	85.84	86.90	79.57	83.07
PromptKD \dagger (CVPR 24)	83.69	81.54	82.60	85.84	71.37	77.94	97.54	82.08	89.14	89.71	82.27	86.10
CoOp + ATPrompt \dagger (ICCV 25)	80.84	68.64	74.24	80.83	45.49	58.22	90.34	59.79	71.96	84.49	64.96	73.45
PromptKD + ATPrompt \dagger (ICCV 25)	83.87	81.35	82.59	86.92	72.34	78.96	97.05	92.07	94.49	89.29	82.44	85.73
CoOp + TIES (NeurIPS 23)	62.41	62.99	62.70	57.33	41.87	48.40	50.17	69.85	58.40	62.45	54.68	58.30
CoOp + DARE (ICML 24)	70.33	63.01	66.47	72.49	47.02	57.04	69.71	65.22	67.39	77.61	57.84	66.28
CoOp + MERGETUNE	80.37	76.19	78.22	78.51	56.84	65.93	85.15	64.51	73.40	82.04	78.33	80.14
KgCoOp + TIES (NeurIPS 23)	73.05	73.88	73.46	60.77	53.54	56.93	68.66	65.45	67.02	74.46	73.91	74.18
KgCoOp + DARE (ICML 24)	77.47	74.81	76.12	72.46	54.19	62.01	84.48	63.03	72.19	81.63	75.99	78.71
KgCoOp + MERGETUNE	80.53	77.28	78.87	79.90	57.33	66.75	89.56	67.89	77.22	83.35	77.76	80.45
MMA + TIES (NeurIPS 23)	69.46	65.77	67.56	55.38	48.36	51.63	65.69	67.95	66.80	71.74	60.42	65.60
MMA + DARE (ICML 24)	71.43	72.61	72.02	67.65	50.37	57.74	77.42	64.16	70.17	78.46	64.47	70.78
MMA + MERGETUNE	82.46	78.48	80.42	83.37	65.34	73.26	90.09	81.91	85.81	86.37	81.02	83.61
PromptKD \dagger + TIES (NeurIPS 23)	79.11	76.49	77.78	78.86	65.93	71.82	88.64	81.59	84.97	82.47	77.32	79.81
PromptKD \dagger + DARE (ICML 24)	80.34	79.66	80.00	84.22	70.04	76.48	92.48	82.11	86.99	86.97	80.68	83.71
PromptKD \dagger + MERGETUNE	83.92	81.49	82.69	86.77	72.10	78.76	97.81	83.82	90.28	89.99	82.79	86.24

Table 2: Cross-dataset generalisation results. Models are trained on ImageNet and directly evaluated on other datasets. Avg-C = average over all cross-dataset targets. *: Our reproduction. \dagger : Using external knowledge.

Method	Caltech101	Oxford Pets	Stanford Cars	Flowers102	Food101	FGVC Aircraft	SUN397	DTD	EuroSAT	UCF101	Avg-C
CLIP (ICML 21)	93.30	89.10	65.70	70.70	85.90	24.90	62.60	44.30	48.30	67.60	65.24
CoOp (IJCV 22)	93.70	89.14	64.51	68.71	85.30	18.47	64.15	41.92	46.39	66.55	63.88
+TIES (NeurIPS 23)	93.31	88.25	65.51	67.40	85.23	23.91	62.56	44.39	42.22	65.24	63.80 <small>(-0.08)</small>
+DARE (ICML 24)	89.67	86.40	62.87	66.32	84.27	18.07	60.27	38.55	45.65	64.68	61.67 <small>(-2.21)</small>
+MERGETUNE	93.96	89.97	65.67	70.40	86.43	23.88	66.35	46.53	46.12	68.71	65.80 <small>(+1.92)</small>
KgCoOp (CVPR 22)	93.92	89.83	65.41	70.01	86.36	22.51	66.16	46.35	46.04	68.50	65.51
+TIES (NeurIPS 23)	91.94	87.56	64.33	66.92	85.53	21.69	63.66	41.75	46.36	65.74	63.55 <small>(-1.96)</small>
+DARE (ICML 24)	93.66	88.15	64.81	69.29	86.16	22.24	64.64	45.09	45.38	66.06	64.55 <small>(-0.96)</small>
+MERGETUNE	94.24	90.41	66.15	70.85	86.57	24.12	66.63	47.46	48.41	70.42	66.53 <small>(+1.02)</small>
MMA* (CVPR 24)	93.80	89.65	65.41	69.86	85.79	24.47	67.31	45.26	43.70	68.82	65.41
+TIES (NeurIPS 23)	90.54	86.21	62.46	65.35	84.21	17.98	60.33	38.35	41.69	64.13	61.13 <small>(-4.28)</small>
+DARE (ICML 24)	91.24	87.14	63.25	66.45	84.43	19.46	62.12	40.44	42.89	65.35	62.28 <small>(-3.13)</small>
+MERGETUNE	94.28	90.43	66.11	71.46	86.26	25.26	67.59	46.22	46.16	69.23	66.30 <small>(+0.89)</small>
PromptKD \dagger (ICLR 24)	93.61	91.59	73.93	75.33	88.84	26.24	68.57	55.08	63.74	76.39	71.33
+TIES (NeurIPS 23)	91.35	89.25	70.35	69.36	86.26	23.74	64.75	50.36	60.68	72.54	67.86 <small>(-3.47)</small>
+DARE (ICML 24)	93.26	90.36	73.26	74.26	88.36	25.14	67.47	54.26	63.03	75.19	70.46 <small>(-0.87)</small>
+MERGETUNE	93.95	92.01	74.17	75.39	89.32	26.58	68.61	55.74	63.94	77.12	71.68 <small>(+0.35)</small>

Few-shot setting. *Base-to-novel generalisation*: We evaluate on 11 datasets, each dataset is split into base and novel classes; models are trained on base classes and evaluated on both base and novel categories, with harmonic mean (HM) reported as the main metric. *Cross-dataset generalisation*: Following (Zhou et al., 2022a), models are trained on ImageNet (16 shots per class) and directly evaluated on other datasets without further adaptation. *Domain generalisation*: To assess robustness to domain shift, it is to evaluate ImageNet-finetuned models on four ImageNet variants.

Many-shot setting. *ID-OOD generalisation*: In the robust learning setting, models are initialized from pre-trained CLIP with an additional linear classifier head derived from CLIP’s zero-shot text embeddings generated by encoding class-specific text prompts through the pre-trained text encoder, then fine-tuned on ImageNet-1K using standard supervised cross-entropy loss. The finetuned model is tested without any additional training or adaptation across both in-distribution and out-of-distribution settings. We report performance on the four domain-shifted ImageNet variants plus ObjectNet (Barbu et al., 2019). All reported results are averaged over three random seeds.

5.1 IMPLEMENTATION DETAILS

Base models. We evaluate our continued fine-tuning strategy on multiple VLM adaptation methods. For few-shot learning, we build upon CoOp (Zhou et al., 2022b), KgCoOp (Yao et al., 2023), MMA (Yang et al., 2024), and PromptKD (Li et al., 2024), while for many-shot settings we consider linear-head and full-model fine-tuning. For each baseline, we reproduce it to obtain a downstream checkpoint. We then apply MERGETUNE to this checkpoint together with the zero-shot CLIP model, following the same training configurations as the respective baseline. All experiments use CLIP ViT-B/16 backbone. Details on datasets, training, and evaluation are in the supplement.

Competitors. We compare our MERGETUNE against two families of competing methods. First, we compare with existing training-free model merging techniques, including TIES (Yadav et al., 2023), which mitigates parameter interference via task-wise sparsification; and DARE (Yu et al., 2024), which improves cross-task transfer through reweighting strategies. Second, we evaluate against representative ensembling approaches: Wise-FT (Wortsman et al., 2022b), which linearly interpolates pretrained and finetuned weights, and VRF (Zhu et al., 2024), which enhances robustness through variance-reduction ensembles. These methods provide strong baselines for assessing the effectiveness of our MERGETUNE.

5.2 FEW-SHOT BASE-TO-NOVEL GENERALISATION

Table 1 reports base-to-novel generalisation across 11 datasets. We extend CoOp, KgCoOp, and PromptKD with training-free model merging methods, including TIES, DARE, and our MERGETUNE. Since training-free merging cannot directly handle models with structural differences (e.g., MMA, whose adapted models differ from pretrained CLIP), we instead merge only the linear heads while preserving the original MMA image encoder.

The results highlight two key observations. First, merging zero-shot and fine-tuned checkpoints via TIES or DARE degrades performance. For example, CoOp+TIES reduces the HM by 5.33% compared to vanilla CoOp, while CoOp+DARE decreases it by 1.07%. Even when applied to stronger baselines such as PromptKD, these training-free approaches fail to improve performance, underscoring the difficulty of directly interpolating between CLIP and fine-tuned checkpoints.

Second, our MERGETUNE consistently improves generalisation across all baselines. The magnitude of improvement correlates inversely with baseline performance, which is theoretically consistent with our framework. Methods that already preserve pretrained knowledge well (e.g., PromptKD at 83.13% HM) have less forgotten knowledge to recover, thus showing smaller but consistent gains (+0.36%). Conversely, methods with more catastrophic forgetting (e.g., CoOp at 71.66% HM) benefit more substantially (+5.58%), as our LMC-based approach has more pretrained knowledge to restore. This demonstrates that MERGETUNE’s effectiveness scales with the degree of forgetting, making it particularly valuable for improving methods that struggle with knowledge retention.

5.3 FEW-SHOT CROSS-DATASET GENERALISATION

Table 2 presents cross-dataset generalisation results, where models trained on ImageNet are directly evaluated on 10 other datasets without adaptation. Training-free merging methods (TIES and DARE) generally degrade performance, whereas MERGETUNE delivers consistent gains across all baselines, with average HM improvements of +1.92 on CoOp, +0.86 on KgCoOp, +0.89 on MMA, and +0.35 on PromptKD. The improvements are especially pronounced on challenging datasets such as FGVC Aircraft, DTD and EuroSAT. Notably, by merging pretrained knowledge from the zero-shot model via our MERGETUNE, MMA is able to surpass CLIP on all evaluated datasets.

5.4 FEW-SHOT DOMAIN GENERALISATION

We evaluate the models few-shot-tuned from ImageNet on various out-of-domain datasets shown in Table 3. Again, training-free merging approaches (TIES and DARE) gain negative performance gains across all baselines, with notable degradation on datasets featuring larger shifts, such as ImageNet-Sketch and ImageNet-Adversarial. Our MERGETUNE consistently outperforms all baselines against domain shifts, achieving positive gains of +0.87 for CoOp, +0.35 for KgCoOp, +0.42 for MMA, and +0.30 for PromptKD (as Avg-D), confirming enhanced robustness under distribution shift scenarios.

Table 3: Domain generalisation results on ImageNet and four distribution shifts. Avg-D = average over domain-shifted datasets. MMA* is our reproduction.

Method	ImageNet	-V2	-S	-A	-R	Avg-D
CoOp (ICCV 22)	71.51	64.20	47.99	49.71	75.21	59.28
+TIES (NeurIPS 23)	62.84	56.26	41.14	44.65	70.77	53.20 (-6.08)
+DARE (ICML 24)	69.02	61.75	45.87	49.10	73.85	57.64 (-1.64)
+MERGETUNE	71.68	64.56	48.67	50.74	76.61	60.15 (+0.87)
KgCoOp (CVPR 22)	70.66	64.10	48.97	50.69	76.70	60.11
+TIES (NeurIPS 23)	67.77	61.47	46.36	49.86	75.91	58.40 (-1.71)
+DARE (ICML 24)	69.67	62.89	47.69	50.33	76.15	59.27 (-0.84)
+MERGETUNE	71.80	64.70	49.10	51.01	77.02	60.46 (+0.35)
MMA* (CVPR 24)	70.45	63.87	48.84	49.91	77.29	59.98
+TIES (NeurIPS 23)	64.01	57.13	42.32	45.23	72.11	54.20 (-5.78)
+DARE (ICML 24)	68.35	58.67	44.75	47.26	74.26	56.24 (-3.74)
+MERGETUNE	71.11	64.41	49.26	50.43	77.51	60.40 (+0.42)
PromptKD [†] (ICLR 24)	77.12	69.77	58.72	70.36	87.01	71.47
+TIES (NeurIPS 23)	74.63	64.22	54.85	67.47	83.85	67.60 (-3.87)
+DARE (ICML 24)	76.14	68.94	56.89	69.36	86.67	70.47 (-1.00)
+MERGETUNE	77.14	70.21	58.97	70.68	87.22	71.77 (+0.30)

5.5 ID-OOD GENERALISATION

Table 4 presents the robust fine-tuning evaluation on ImageNet and five datasets under distribution shifts. We repurposed model merging methods for this evaluation. However, training-free merging methods, TIES and DARE, exhibit unstable performance and severe degradation under challenging shifts. Our MERGETUNE outperforms SOTA ensembling methods, such as VRF. Notably, MER-

Table 4: ID-OOD generalisation accuracy of various methods on ImageNet and distribution shifts for CLIP ViT-B/16 in the robust fine-tuning evaluation. Avg-D = average over domain-shifted datasets.

Method	Imagenet	Distribution shifts					Avg-D
		-V2	-S	-A	-R	ObjectNet	
Zero-shot (CLIP)	68.34	61.90	48.27	50.12	77.60	54.23	58.42
Linear Probing (CVPR 22)	79.79	70.02	46.99	46.48	71.16	52.28	57.39
+ Weight ens. (CVPR 22)	79.80	70.45	48.41	47.89	73.00	53.07	58.56 (+1.17)
+ VRF (NeurIPS 24)	79.84	70.36	48.67	48.08	73.87	53.36	58.87 (+1.48)
+ TIES (NeurIPS 23)	79.75	70.33	48.25	48.32	73.78	53.13	58.76 (+1.37)
+ DARE (ICML 24)	79.14	70.26	48.14	47.74	73.11	53.01	58.45 (+1.06)
+ MERGETUNE	79.96	70.22	49.47	49.21	75.98	53.43	59.66 (+2.27)
+ Weight ens.	79.88	70.27	50.14	50.04	76.69	54.01	60.23 (+2.84)
E2E-FT (CVPR 22)	81.31	70.61	45.12	36.62	65.63	50.51	53.70
+ Weight ens. (CVPR 22)	82.51	73.11	51.62	47.61	75.13	55.71	60.64 (+6.94)
+ VRF (NeurIPS 24)	82.32	72.12	52.93	48.41	78.72	56.41	61.72 (+8.02)
+ TIES (NeurIPS 23)	82.27	72.84	51.67	47.81	74.48	54.87	60.33 (+6.63)
+ DARE (ICML 24)	81.09	70.21	45.79	35.55	65.23	50.13	53.38 (-0.32)
+ MERGETUNE	82.26	72.98	52.76	51.61	78.01	56.22	62.29 (+8.59)
+ Weight ens.	82.18	73.21	53.10	52.68	78.68	56.84	62.90 (+9.20)

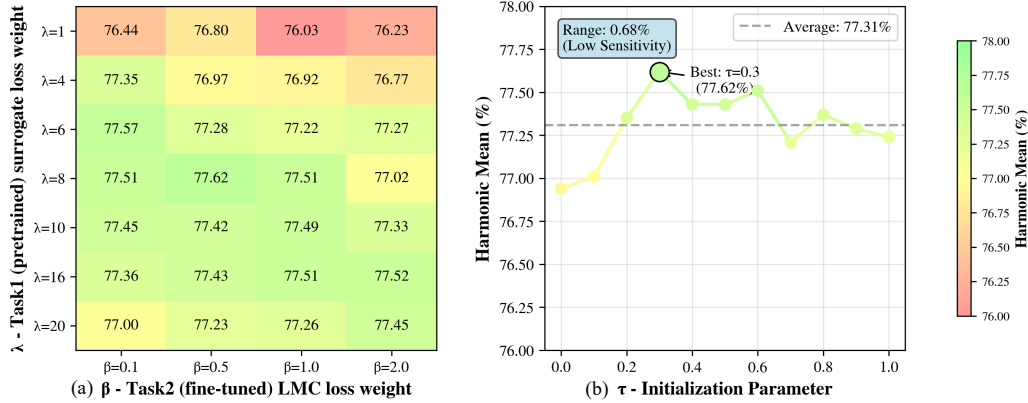


Figure 3: Hyperparameter sensitivity analysis: HM averaged over 11 datasets. (a) Surrogate loss weight λ and Task2 LMC loss weight β . (b) Initialisation parameter τ of the continued model on performance (under $\lambda = 8.0$, $\beta = 0.5$), where $\tau = 0$ means using CLIP weights for initialisation and $\tau = 1$ means using the fine-tuned weights (e.g. KgCoOp here).

GETUNE employs a single model for inference, eliminating the need for failure set construction or per-sample distance computations, which can incur additional inference costs as VRF did.

Furthermore, when combined with weight-space ensembling — which interpolates parameters between the zero-shot and our LMC-tuned checkpoint using a single mixing weight — our MERGETUNE achieves the highest average OOD accuracies: 60.23 (Linear Probing) and 62.90 (E2E-FT). This demonstrates that the LMC-tuned model is a superior replacement for standard fine-tuned checkpoints in ensemble schemes. These results establish our achievement on better ID-OOD trade-offs without complex design, while for the first time outperforming CLIP in all cases.

5.6 FURTHER ANALYSIS

We evaluate the sensitivity of MERGETUNE to key hyper-parameters, including surrogate loss weight λ , Task2 LMC loss weight β , and the initialisation of the continued model. We conduct this ablation averaged over 11 datasets using our method based on KgCoOp initialisation. Figure 3(a) demonstrates that our method is robust to hyperparameter choices, with harmonic mean performance varying within a narrow range across different λ and β combinations. Optimal performance is achieved when $\lambda \in [8, 16]$ and $\beta \in [0.1, 0.5]$, resulting in balanced loss values between different terms. Figure 3(b) shows the impact of the initialisation of the parameters for continued fine-tuning. Given both fine-tuned and zero-shot checkpoints, we initialise the parameters by merging them as $w = (1 - \tau)\hat{w}_1 + \tau\hat{w}_2$, $\tau \in [0, 1]$, where $\tau = 0$ corresponds to CLIP weights and $\tau = 1$ to fine-tuned weights. When the initialisation combines CLIP and the fine-tuned model in a balanced manner ($\tau \in [0.3, 0.6]$), performance remains optimal.

6 CONCLUSION

We introduced continued fine-tuning (CFT), a new paradigm that recovers pretrained knowledge of a task-adapted VLM. Our method, MERGETUNE, searches for a continued model that is linear-mode connected to zero-shot and fine-tuned checkpoints, thus effectively integrating their knowledge. MERGETUNE is model-agnostic and can be applied post hoc to existing fine-tuned VLMs, without requiring architectural changes. Experimental results on base-to-novel, cross-dataset, domain generalisation, and robust fine-tuning benchmarks all showed the efficacy of our MERGETUNE, establishing continued fine-tuning as a promising direction for advancing VLM adaptation.

REFERENCES

Andrei Barbu, David Mayo, Julian Alverio, William Luo, Christopher Wang, Dan Gutfreund, Josh Tenenbaum, and Boris Katz. Objectnet: A large-scale bias-controlled dataset for pushing the limits of object recognition models. *Advances in Neural Information Processing Systems (NeurIPS)*, 32, 2019.

Lukas Bossard, Matthieu Guillaumin, and Luc Van Gool. Food-101–mining discriminative components with random forests. In *European conference on computer vision (ECCV)*, pp. 446–461. Springer, 2014.

Mircea Cimpoi, Subhransu Maji, Iasonas Kokkinos, Sammy Mohamed, and Andrea Vedaldi. Describing textures in the wild. In *IEEE/CVF Conference on Computer Vision and Pattern Recognition (CVPR)*, pp. 3606–3613, 2014.

Jia Deng, Wei Dong, Richard Socher, Li-Jia Li, Kai Li, and Li Fei-Fei. Imagenet: A large-scale hierarchical image database. In *IEEE/CVF Conference on Computer Vision and Pattern Recognition (CVPR)*, pp. 248–255, 2009.

Felix Draxler, Kambis Veschgini, Manfred Salmhofer, and Fred Hamprecht. Essentially no barriers in neural network energy landscape. In *International conference on machine learning (ICML)*, pp. 1309–1318. PMLR, 2018.

Li Fei-Fei, Rob Fergus, and Pietro Perona. Learning generative visual models from few training examples: An incremental bayesian approach tested on 101 object categories. In *IEEE/CVF Conference on Computer Vision and Pattern Recognition (CVPR) workshop*, pp. 178–178. IEEE, 2004.

Peng Gao, Shijie Geng, Renrui Zhang, Teli Ma, Rongyao Fang, Yongfeng Zhang, Hongsheng Li, and Yu Qiao. Clip-adapter: Better vision-language models with feature adapters. *International Journal of Computer Vision (IJCV)*, 132(2):581–595, 2024.

Timur Garipov, Pavel Izmailov, Dmitrii Podoprikhin, Dmitry P Vetrov, and Andrew G Wilson. Loss surfaces, mode connectivity, and fast ensembling of dnns. *Advances in Neural Information Processing Systems (NeurIPS)*, 31, 2018.

Patrick Helber, Benjamin Bischke, Andreas Dengel, and Damian Borth. Eurosat: A novel dataset and deep learning benchmark for land use and land cover classification. *IEEE Journal of Selected Topics in Applied Earth Observations and Remote Sensing*, 12(7):2217–2226, 2019.

Dan Hendrycks, Steven Basart, Norman Mu, Saurav Kadavath, Frank Wang, Evan Dorundo, Rahul Desai, Tyler Zhu, Samyak Parajuli, Mike Guo, et al. The many faces of robustness: A critical analysis of out-of-distribution generalization. In *International Conference on Computer Vision (ICCV)*, pp. 8340–8349, 2021a.

Dan Hendrycks, Kevin Zhao, Steven Basart, Jacob Steinhardt, and Dawn Song. Natural adversarial examples. In *IEEE/CVF Conference on Computer Vision and Pattern Recognition (CVPR)*, pp. 15262–15271, 2021b.

Chenyu Huang, Peng Ye, Tao Chen, Tong He, Xiangyu Yue, and Wanli Ouyang. Emr-merging: Tuning-free high-performance model merging. In *Advances in Neural Information Processing Systems (NeurIPS)*, 2024.

Gabriel Ilharco, Marco Tulio Ribeiro, Mitchell Wortsman, Suchin Gururangan, Ludwig Schmidt, Hannaneh Hajishirzi, and Ali Farhadi. Editing models with task arithmetic. In *International Conference on Learning Representations (ICLR)*, 2023.

Pavel Izmailov, Dmitrii Podoprikhin, Timur Garipov, Dmitry Vetrov, and Andrew Gordon Wilson. Averaging weights leads to wider optima and better generalization. *arXiv preprint arXiv:1803.05407*, 2018.

Haojun Jiang, Jianke Zhang, Rui Huang, Chunjiang Ge, Zanlin Ni, Jiwen Lu, Jie Zhou, Shiji Song, and Gao Huang. Cross-modal adapter for text-video retrieval. *Pattern Recognition*, 2025.

Muhammad Uzair Khattak, Hanoona Rasheed, Muhammad Maaz, Salman Khan, and Fahad Shahbaz Khan. Maple: Multi-modal prompt learning. In *IEEE/CVF Conference on Computer Vision and Pattern Recognition (CVPR)*, pp. 19113–19122, 2023.

Sungyeon Kim, Boseung Jeong, Donghyun Kim, and Suha Kwak. Efficient and versatile robust fine-tuning of zero-shot models. In *European conference on computer vision (ECCV)*, pp. 440–458. Springer, 2024.

Jonathan Krause, Michael Stark, Jia Deng, and Li Fei-Fei. 3d object representations for fine-grained categorization. In *International Conference on Computer Vision (ICCV) workshop*, pp. 554–561, 2013.

Ananya Kumar, Aditi Raghunathan, Robbie Jones, Tengyu Ma, and Percy Liang. Fine-tuning can distort pretrained features and underperform out-of-distribution. In *International Conference on Learning Representations (ICLR)*, 2022.

Balaji Lakshminarayanan, Alexander Pritzel, and Charles Blundell. Simple and scalable predictive uncertainty estimation using deep ensembles. In *Advances in Neural Information Processing Systems (NeurIPS)*, 2017.

Zheng Li, Xiang Li, Xinyi Fu, Xin Zhang, Weiqiang Wang, Shuo Chen, and Jian Yang. Prompttkd: Unsupervised prompt distillation for vision-language models. In *IEEE/CVF Conference on Computer Vision and Pattern Recognition (CVPR)*, pp. 26617–26626, 2024.

Zheng Li, Yibing Song, Ming-Ming Cheng, Xiang Li, and Jian Yang. Advancing textual prompt learning with anchored attributes. In *International Conference on Computer Vision (ICCV)*, 2025.

Yuning Lu, Jianzhuang Liu, Yonggang Zhang, Yajing Liu, and Xinmei Tian. Prompt distribution learning. In *IEEE/CVF Conference on Computer Vision and Pattern Recognition (CVPR)*, pp. 5206–5215, 2022.

Subhransu Maji, Esa Rahtu, Juho Kannala, Matthew Blaschko, and Andrea Vedaldi. Fine-grained visual classification of aircraft. *arXiv preprint arXiv:1306.5151*, 2013.

Seyed Iman Mirzadeh, Mehrdad Farajtabar, Dilan Gorur, Razvan Pascanu, and Hassan Ghasemzadeh. Linear mode connectivity in multitask and continual learning. In *International Conference on Learning Representations (ICLR)*, 2021.

Maria-Elena Nilsback and Andrew Zisserman. Automated flower classification over a large number of classes. In *2008 Sixth Indian conference on computer vision, graphics & image processing*, pp. 722–729. IEEE, 2008.

Omkar M Parkhi, Andrea Vedaldi, Andrew Zisserman, and CV Jawahar. Cats and dogs. In *IEEE/CVF Conference on Computer Vision and Pattern Recognition (CVPR)*, pp. 3498–3505. IEEE, 2012.

Adam Paszke, Sam Gross, Francisco Massa, Adam Lerer, James Bradbury, Gregory Chanan, Trevor Killeen, Zeming Lin, Natalia Gimelshein, Luca Antiga, et al. Pytorch: An imperative style, high-performance deep learning library. In *Advances in Neural Information Processing Systems (NeurIPS)*, pp. 8026–8037, 2019.

Alec Radford, Jong Wook Kim, Chris Hallacy, Aditya Ramesh, Gabriel Goh, Sandhini Agarwal, Girish Sastry, Amanda Askell, Pamela Mishkin, Jack Clark, et al. Learning transferable visual models from natural language supervision. In *International conference on machine learning (ICML)*, pp. 8748–8763. PMLR, 2021.

Benjamin Recht, Rebecca Roelofs, Ludwig Schmidt, and Vaishaal Shankar. Do imagenet classifiers generalize to imagenet? In *International conference on machine learning (ICML)*, pp. 5389–5400. PMLR, 2019.

Khurram Soomro, Amir Roshan Zamir, and Mubarak Shah. Ucf101: A dataset of 101 human actions classes from videos in the wild. *arXiv preprint arXiv:1212.0402*, 2012.

Michael Tschannen, Alexey Gritsenko, Xiao Wang, Muhammad Ferjad Naeem, Ibrahim Alabdulmohsin, Nikhil Parthasarathy, Talfan Evans, Lucas Beyer, Ye Xia, Basil Mustafa, et al. Siglip 2: Multilingual vision-language encoders with improved semantic understanding, localization, and dense features. *arXiv preprint arXiv:2502.14786*, 2025.

Haohan Wang, Songwei Ge, Zachary Lipton, and Eric P Xing. Learning robust global representations by penalizing local predictive power. *Advances in Neural Information Processing Systems (NeurIPS)*, 32, 2019.

Mitchell Wortsman, Gabriel Ilharco, Samir Ya Gadre, Rebecca Roelofs, Raphael Gontijo-Lopes, Ari S Morcos, Hongseok Namkoong, Ali Farhadi, Yair Carmon, Simon Kornblith, et al. Model soups: averaging weights of multiple fine-tuned models improves accuracy without increasing inference time. In *International conference on machine learning (ICML)*, pp. 23965–23998. PMLR, 2022a.

Mitchell Wortsman, Gabriel Ilharco, Jong Wook Kim, Mike Li, Simon Kornblith, Rebecca Roelofs, Raphael Gontijo Lopes, Hannaneh Hajishirzi, Ali Farhadi, Hongseok Namkoong, et al. Robust fine-tuning of zero-shot models. In *IEEE/CVF Conference on Computer Vision and Pattern Recognition (CVPR)*, pp. 7959–7971, 2022b.

Jianxiong Xiao, James Hays, Krista A Ehinger, Aude Oliva, and Antonio Torralba. Sun database: Large-scale scene recognition from abbey to zoo. In *IEEE/CVF Conference on Computer Vision and Pattern Recognition (CVPR)*, pp. 3485–3492. IEEE, 2010.

Prateek Yadav, Derek Tam, Leshem Choshen, Colin A Raffel, and Mohit Bansal. Ties-merging: Resolving interference when merging models. *Advances in Neural Information Processing Systems (NeurIPS)*, 36:7093–7115, 2023.

Lingxiao Yang, Ru-Yuan Zhang, Yanchen Wang, and Xiaohua Xie. Mma: Multi-modal adapter for vision-language models. In *IEEE/CVF Conference on Computer Vision and Pattern Recognition (CVPR)*, pp. 23826–23837, 2024.

Hantao Yao, Rui Zhang, and Changsheng Xu. Visual-language prompt tuning with knowledge-guided context optimization. In *IEEE/CVF Conference on Computer Vision and Pattern Recognition (CVPR)*, pp. 6757–6767, 2023.

Hantao Yao, Rui Zhang, and Changsheng Xu. Tcp: Textual-based class-aware prompt tuning for visual-language model. In *IEEE/CVF Conference on Computer Vision and Pattern Recognition (CVPR)*, pp. 23438–23448, 2024.

Le Yu, Bowen Yu, Haiyang Yu, Fei Huang, and Yongbin Li. Language models are super mario: Absorbing abilities from homologous models as a free lunch. In *International conference on machine learning (ICML)*, 2024.

Yuhang Zang, Wei Li, Kaiyang Zhou, Chen Huang, and Chen Change Loy. Unified vision and language prompt learning. *arXiv preprint arXiv:2210.07225*, 2022.

Renrui Zhang, Wei Zhang, Rongyao Fang, Peng Gao, Kunchang Li, Jifeng Dai, Yu Qiao, and Hongsheng Li. Tip-adapter: Training-free adaption of clip for few-shot classification. In *European conference on computer vision (ECCV)*, pp. 493–510. Springer, 2022.

Kaiyang Zhou, Jingkang Yang, Chen Change Loy, and Ziwei Liu. Conditional prompt learning for vision-language models. In *IEEE/CVF Conference on Computer Vision and Pattern Recognition (CVPR)*, 2022a.

Kaiyang Zhou, Jingkang Yang, Chen Change Loy, and Ziwei Liu. Learning to prompt for vision-language models. *International Journal of Computer Vision (IJCV)*, 2022b.

Kaiyang Zhou, Ziwei Liu, Yu Qiao, Tao Xiang, and Chen Change Loy. Domain generalization: A survey. *IEEE Transactions on Pattern Analysis and Machine Intelligence*, 45(4):4396–4415, 2023. doi: 10.1109/TPAMI.2022.3195549.

Beier Zhu, Jiequan Cui, and Hanwang Zhang. Robust fine-tuning of zero-shot models via variance reduction. *Advances in Neural Information Processing Systems (NeurIPS)*, 37:76967–76990, 2024.

A APPENDIX

A.1 EXPERIMENTAL SETTINGS

Our framework is implemented in PyTorch Paszke et al. (2019), and all experiments are conducted on an NVIDIA 3090 GPU.

Few-shot setting To evaluate MERGETUNE, we apply it to the following base methods: the prompt learning methods CoOp (Zhou et al., 2022b) and KgCoOp (Yao et al., 2023), the adapter-based method MMA (Yang et al., 2024), and the distillation-based method PromptKD (Li et al., 2024). For each base method, we first reproduce the fine-tuning procedure to obtain a downstream checkpoint. Our MERGETUNE is then applied to this checkpoint in conjunction with the zero-shot CLIP model. Following the baselines, we adopt a standard data augmentation scheme of random resized cropping and flipping. We use Stochastic Gradient Descent (SGD) as the optimizer. The number of prompt context tokens is set to 4, initialised as “*a photo of a []*”. All few-shot experiments are trained with 16 shots.

CoOp + MERGETUNE. Following the baseline, we use a batch size of 128 and an initial learning rate of 0.002 for the first round of downstream training over 100 epochs. Our MERGETUNE is then trained for 50 epochs using the same optimiser and training schedule as the base method.

KgCoOp + MERGETUNE. KgCoOp follows the same training epochs, schedule, and data augmentation settings as CoOp. The regularisation weight is set to $\lambda=8.0$, as in the original configuration. Our MERGETUNE reuses the same training setup as the baseline.

MMA + MERGETUNE. Following the baseline, we insert the multi-modal unit from transformer block $k=5$ to the final block in both the language and vision branches, with a shared projection dimension of 32. In the base to novel generalisation, models are trained for 5 epochs with a batch size of 128 on ImageNet and 16 on the other ten datasets. For the other experimental settings, we set $k=9$ and train for only one epoch. Training is performed with mixed precision, and our MERGETUNE follows the same training schedule and number of epochs as the baseline for each dataset.

PromptKD + MERGETUNE. We use publicly available pre-trained teacher models and train student models for 20 epochs with a batch size of 8 and a learning rate of 0.005. Our MERGETUNE follows the same training schedule.

Many-shot setting For robust finetuning, we apply MERGETUNE to both linear probing and end-to-end fine-tuning (E2E-FT). Same as in the few-shot setting, we first fine-tune CLIP to obtain finetuned checkpoints, and then apply MERGETUNE to derive results.

Linear probing. We train only the classifier head for 10 epochs using SGD with a learning rate of 1×10^{-2} , batch size 512, and a cosine learning-rate schedule.

End-to-end Fine-tuning. We jointly update the encoder and classifier head for 10 epochs using AdamW with a learning rate of 3×10^{-5} , batch size 512, weight decay 0.05, and a cosine learning rate schedule with warmup. After obtaining the fine-tuned checkpoint, we apply MERGETUNE for the same number of epochs, reusing the corresponding optimiser and training schedule.

Datasets We evaluate the **few-shot setting** on various settings. For generalisation from *base-to-novel* classes and *cross-dataset evaluation*, we test our method on 11 diverse recognition datasets. Specifically, these include ImageNet-1K Deng et al. (2009) and Caltech-101 Fei-Fei et al. (2004) for generic object classification; OxfordPets Parkhi et al. (2012), StanfordCars Krause et al. (2013), Flowers-102 Nilsback & Zisserman (2008), Food-101 Bossard et al. (2014), and FGVC Aircraft Maji et al. (2013) for fine-grained classification; SUN-397 Xiao et al. (2010) for scene recognition; UCF-101 Soomro et al. (2012) for action recognition; DTD Cimpoi et al. (2014) for texture classification; and EuroSAT Helber et al. (2019) for satellite imagery recognition. For *domain generalisation* experiments, we use ImageNet-1K Deng et al. (2009) as the source dataset and its four variants as target datasets: ImageNet-V2 Recht et al. (2019), ImageNet-Sketch Wang et al. (2019), ImageNet-A Hendrycks et al. (2021b), and ImageNet-R Hendrycks et al. (2021a).

For the **many-shot setting**, we report results on ImageNet Deng et al. (2009) and its five distribution-shift variants: (1) ImageNet-V2 (-V2) Recht et al. (2019): test images sampled a decade after the original ImageNet. (2) ImageNet-R (-R) Hendrycks et al. (2021a): contains renditions (e.g., art, cartoons, graffiti). (3) ImageNet-Sketch (-S) Wang et al. (2019): consists of sketches instead of natural photos. (4) ImageNet-A (-A) Hendrycks et al. (2021b): real-world images that are misclassified by ResNet models. (5) ObjectNet Barbu et al. (2019): a test set featuring objects with diverse backgrounds, rotations, and viewpoints.

A.2 PSEUDO-CODE

Algorithm 1 Continued finetuning — MERGETUNE

```

1: Input: zero-shot weights  $\hat{w}_1$ , fine-tuned weights  $\hat{w}_2$ , downstream dataset  $\mathcal{D}_2$ , downstream task
   loss  $\mathcal{L}_2(\cdot)$ , surrogate loss weight  $\lambda$ , LMC loss weight  $\beta$ , number of interpolation points  $n$ ,
   initialisation coefficient  $\tau$ 
2: Output: continued model weights  $w$ 
3:  $A \leftarrow \{1/n, 2/n, \dots, (n-1)/n\}$ 
4: Initialise  $w \leftarrow (1 - \tau)\hat{w}_1 + \tau\hat{w}_2$             $\triangleright w$  is initialised by blending zero-shot and fine-tuned
   weights.
5: for each training epoch do
6:   for each minibatch  $(x, y)$  from  $\mathcal{D}_2$  do
7:      $\mathcal{L}_{\text{task}} \leftarrow \mathcal{L}_2(w; x, y)$             $\triangleright$  Downstream task loss
8:      $\mathcal{L}_{\text{sur}} \leftarrow \|w - \hat{w}_1\|^2$             $\triangleright$  Surrogate loss for Task 1
9:      $\mathcal{L}_{\text{LMC}} \leftarrow 0$ 
10:    for each  $\alpha \in A$  do
11:       $w_{\text{interp}} \leftarrow \hat{w}_2 + \alpha(w - \hat{w}_2)$ 
12:       $\mathcal{L}_{\text{LMC}} \leftarrow \mathcal{L}_{\text{LMC}} + \mathcal{L}_2(w_{\text{interp}}; x, y)$ 
13:    end for
14:     $\mathcal{L}_{\text{LMC}} \leftarrow \mathcal{L}_{\text{LMC}}/|A|$             $\triangleright$  Average LMC loss
15:     $\mathcal{J} \leftarrow \mathcal{L}_{\text{task}} + \lambda\mathcal{L}_{\text{sur}} + \beta\mathcal{L}_{\text{LMC}}$ 
16:    Update  $w$  with SGD step on  $\mathcal{J}$ 
17:  end for
18: end for
19: return  $w$ 

```

A.3 ADDITIONAL EXPERIMENTS

A.3.1 GENERALISATION TO OTHER BACKBONES

We also evaluate our MERGETUNE with other backbones to test its generalisation. We report results in Table 5 using CLIP ViT-B/32, which was commonly used in prior robust fine-tuning works (Zhu et al., 2024; Kim et al., 2024). The conclusion is consistent with the results in Table 4.

To further evaluate the scalability of MERGETUNE, we conduct experiments with three additional vision-language model backbones: CLIP-L/14, Siglip2-B/16, and Siglip2-L/16 (Tschannen et al., 2025). We compare the base CoOp method with CoOp+MERGETUNE across all 11 datasets for the base-to-novel generalisation evaluation. As shown in Table 6, our method consistently improves performance with new model scales and architectures, demonstrating strong scalability and model-agnostic effectiveness that generalises well beyond specific model architectures.

A.3.2 HYPERPARAMETER EVALUATION

We evaluate the sensitivity of MERGETUNE to key hyper-parameters, including surrogate loss weight λ , Task2 LMC loss weight β , and the initialisation parameter of the continued model. Here is the detailed experimental results. Detailed experimental results are provided in Table 7 and Table 8.

Table 5: ID-OOD generalisation accuracy of various methods on ImageNet and distribution shifts for CLIP ViT-B/32 in the robust fine-tuning evaluation. Avg-D = average over domain-shifted datasets.

Method	Imagenet	Distribution shifts					Avg-D
		-V2	-S	-A	-R	ObjectNet	
Zero-shot (CLIP)	63.34	55.94	42.33	31.45	69.26	43.46	48.49
E2E-FT (CVPR 22)	76.21	64.21	39.62	20.35	57.38	39.63	44.24
+ Weight ens. (CVPR 22)	77.62	66.86	45.67	28.21	66.68	44.72	50.43 (6.19)
+ VRF (NeurIPS 24)	77.60	66.70	47.00	29.20	70.90	46.30	52.02 (7.78)
+ TIES (NeurIPS 23)	77.20	65.88	46.20	28.12	69.21	44.56	50.79 (6.55)
+ DARE (ICML 24)	77.43	66.32	46.49	28.55	69.75	45.13	51.25 (7.01)
+ MERGETUNE	77.81	67.02	46.83	31.80	70.67	47.01	52.67 (8.43)
+ Weight ens.	77.27	66.59	46.87	32.40	71.09	46.99	52.79 (8.55)

Table 6: Base-to-novel generalisation experiments across different vision-language models on 11 datasets. Our method achieves consistent performance improvement over CoOp baseline across all model architectures.

Method	Average			ImageNet			Caltech101			OxfordPets		
	Base	Novel	HM	Base	Novel	HM	Base	Novel	HM	Base	Novel	HM
<i>CLIP-L14</i>												
CoOp	86.61	74.69	80.21	82.01	71.80	76.57	98.66	96.07	97.35	96.08	98.36	97.21
CoOp + MERGETUNE	85.90	78.70	82.14 (1.93)	81.93	75.57	78.62	97.59	98.00	97.79	96.64	98.32	97.47
<i>Siglip2-B16</i>												
CoOp	78.31	79.02	78.66	79.97	77.38	78.66	98.52	97.82	98.17	95.85	97.97	96.90
CoOp + MERGETUNE	80.75	79.79	80.26 (1.60)	80.03	77.18	78.58	98.56	97.82	98.19	96.12	98.04	97.07
<i>Siglip2-L16</i>												
CoOp	81.56	83.31	82.43	84.01	80.33	82.13	98.34	98.03	98.19	97.79	98.71	98.25
CoOp + MERGETUNE	83.04	84.43	83.73 (1.30)	84.31	80.42	82.32	98.90	98.23	98.56	97.33	98.41	97.87
Method	StanfordCars			Flowers102			Food101			FGVCAircraft		
	Base	Novel	HM	Base	Novel	HM	Base	Novel	HM	Base	Novel	HM
<i>CLIP-L14</i>												
CoOp	82.72	82.89	82.81	98.96	75.04	85.35	93.46	93.55	93.51	52.64	32.95	40.53
CoOp + MERGETUNE	82.49	83.81	83.14	97.59	79.77	87.79	94.01	94.96	94.48	50.28	42.73	46.20
<i>Siglip2-B16</i>												
CoOp	86.18	96.23	90.93	89.68	85.37	87.47	92.24	93.42	92.83	29.87	39.79	34.12
CoOp + MERGETUNE	86.24	96.26	90.98	92.40	86.33	89.27	92.49	93.51	93.00	31.39	40.19	35.25
<i>Siglip2-L16</i>												
CoOp	90.34	97.58	93.82	92.72	87.28	89.91	94.75	95.51	95.13	35.91	54.63	43.34
CoOp + MERGETUNE	90.66	97.50	93.96	93.42	87.34	90.28	95.11	95.53	95.32	36.03	59.23	44.80
Method	SUN397			DTD			EuroSAT			UCF101		
	Base	Novel	HM	Base	Novel	HM	Base	Novel	HM	Base	Novel	HM
<i>CLIP-L14</i>												
CoOp	84.67	72.33	78.02	82.49	59.50	69.13	93.40	64.94	76.61	87.63	74.16	80.33
CoOp + MERGETUNE	85.87	73.31	79.10	80.82	62.45	70.46	92.33	77.20	84.09	85.37	79.55	82.41
<i>Siglip2-B16</i>												
CoOp	83.27	70.81	76.54	77.35	69.81	73.39	56.75	58.17	57.45	71.72	82.40	76.69
CoOp + MERGETUNE	84.87	72.31	78.09	79.98	72.06	75.81	68.38	60.30	64.09	77.75	83.65	80.59
<i>Siglip2-L16</i>												
CoOp	84.97	74.11	79.17	78.93	72.62	75.65	61.26	70.10	65.38	78.16	87.56	82.59
CoOp + MERGETUNE	85.87	75.16	80.16	81.10	78.26	79.65	70.56	70.59	70.58	80.17	88.05	83.92

A.3.3 SENSITIVITY TO INTERPOLATION NUMBER N_α

To better understand our MERGETUNE, we conducted additional analysis. In Table 9, we varied the number of interpolation points N_α , which is used to approximate the LMC expectation term. Performance improves consistently as N_α increases from 1 to 10, after which it saturates. Meanwhile, the training time gradually increases with scaling N_α up: when using KgCoOp+MERGETUNE, the cost

Table 7: Hyperparameter sensitivity analysis: all reported accuracies are averaged over 11 datasets, across surrogate loss weight λ and Task2 LMC loss weight β .

Parameters		Performance (%)		
λ	β	Avg Base Acc	Avg New Acc	Avg Harmonic Mean
1	0.1	82.86	70.94	76.44
	0.5	82.74	71.66	76.80
	1	82.89	70.22	76.03
	2	82.75	70.67	76.23
4	0.1	82.38	72.90	77.35
	0.5	82.47	72.15	76.97
	1	82.64	71.94	76.92
	2	82.70	71.63	76.77
6	0.1	82.31	73.34	77.57
	0.5	82.41	72.76	77.28
	1	82.56	72.53	77.22
	2	82.80	72.43	77.27
8	0.1	82.04	73.45	77.51
	0.5	82.11	73.60	77.62
	1	82.39	73.18	77.51
	2	82.64	72.11	77.02
10	0.1	81.68	73.64	77.45
	0.5	82.02	73.31	77.42
	1	82.20	73.29	77.49
	2	82.58	72.72	77.33
16	0.1	80.96	74.06	77.36
	0.5	81.42	73.82	77.43
	1	81.65	73.76	77.51
	2	82.10	73.43	77.52
20	0.1	79.93	74.27	77.00
	0.5	80.54	74.18	77.23
	1	80.88	73.95	77.26
	2	81.78	73.55	77.45

Table 8: Initialisation analysis of continued model: performance comparison across 11 datasets with $\lambda = 8.0$ and $\beta = 0.5$. Here, $\tau = 0$ corresponds to initialising the continued model with the CLIP weights, while $\tau = 1$ corresponds to the finetuned KgCoOp weights.

τ	Base Acc	New Acc	Harmonic Mean
0.0	81.24	73.07	76.94
0.1	81.47	73.01	77.01
0.2	81.84	73.33	77.35
0.3	82.11	73.60	77.62
0.4	81.91	73.41	77.43
0.5	82.01	73.34	77.43
0.6	82.10	73.42	77.51
0.7	82.07	72.90	77.21
0.8	82.15	73.13	77.37
0.9	82.03	73.07	77.29
1.0	82.16	72.87	77.24

is about $3\times$ that of KgCoOp at $N_\alpha = 5$, increases to $5\times$ at $N_\alpha = 10$, and reaches $7\times$ at $N_\alpha = 15$. Thus, although $N_\alpha = 10$ provides a slight further improvement in accuracy, the associated overhead is more noticeable, making $N_\alpha = 5$ a more balanced choice.

Second, in Table 10, we examined the role of the downstream task loss $L_2(w)$ in Eq. 9. We adopt the decoupled formulation where $L_2(w)$ (at $\alpha = 1$) is assigned full weight outside the expectation. This design ensures that the deployed model w always receives strong endpoint supervision, preserving base-class specialization and yielding a higher harmonic mean. In contrast, if $L_2(w)$ is included inside the expectation, its effective weight is reduced to β and diluted over intermediate interpolations, which weakens base performance. Therefore, excluding $L_2(w)$ preserves this supervision (weight = 1), maintaining stronger base performance at only a slight cost to novel adaptation.

Third, in Table 11, we analyzed the individual contributions of each loss component by setting $\lambda = 0$ and $\beta = 0$ separately. When $\beta = 0$, the LMC constraint is removed and our method reduces to KgCoOp baseline in prompt learning setting. When $\lambda = 0$, eliminating the surrogate loss that maintains proximity to the zero-shot CLIP model, novel class accuracy drops catastrophically while base accuracy remains high, demonstrating severe overfitting to base classes. This confirms that the zero-shot proximity constraint (λ) is essential for preserving pretrained generalization capability, while the LMC term (β) enables effective integration of task-specific knowledge. Both components are necessary for MERGETUNE to successfully recover forgotten pretrained knowledge while maintaining downstream adaptation.

Table 9: Effect of the number of interpolation points (α) in the LMC approximation. Results are averaged over 11 datasets using MERGETUNE with KgCoOp weights. Performance improves steadily as α increases from 1 to 5, beyond which accuracy saturates and further increases in α only raise fine-tuning cost.

Number of Interpolation Points (N_α)	Base Acc	New Acc	Harmonic Mean
1	81.75	73.12	77.19
3	82.01	73.51	77.53
5	82.11	73.60	77.62
10	82.13	73.71	77.69
15	82.13	73.72	77.70

Table 10: Ablation study on the treatment of the downstream task loss $L_2(w)$ in Eq. 9. Excluding $L_2(w)$ from the expectation (weight = 1) yields better results. In contrast, including $L_2(w)$ in the expectation (weight = β) degrades performance, falling below even KgCoOp initialisation. Results are averaged over 11 datasets with KgCoOp initialisation.

Formulation of $L_2(w)$	Base Acc	New Acc	Harmonic Mean
Included in expectation (weight = β)	79.48	74.26	76.78
Excluded from expectation (weight = 1)	82.11	73.60	77.62

Table 11: Ablation study of loss function components in MERGETUNE. When $\lambda = 0$, the surrogate loss connecting to the zero-shot CLIP model is removed, causing severe degradation in novel class performance. When $\beta = 0$, the LMC constraint is removed and the method reduces to KgCoOp (in prompt learning task). Results are averaged over 11 datasets with KgCoOp initialisation.

Setting	Base Acc	Novel Acc	HM	Note
$\beta = 0$	80.73	73.61	77.01	No LMC constraint
$\lambda = 0$	83.39	61.86	71.03	No surrogate loss
Full MERGETUNE	82.11	73.60	77.62	Both components active

A.3.4 PERFORMANCE OF INTERPOLATED MODELS

We also evaluate the interpolated models between our continued model and the original zero-shot CLIP, as well as between it and the initially fine-tuned KgCoOp model on the base-to-novel setting. As shown in Figure 4, the results demonstrate smooth, low-loss (high-accuracy illustrated) paths between our continued model and both endpoints. Interpolation with the fine-tuned KgCoOp (blue

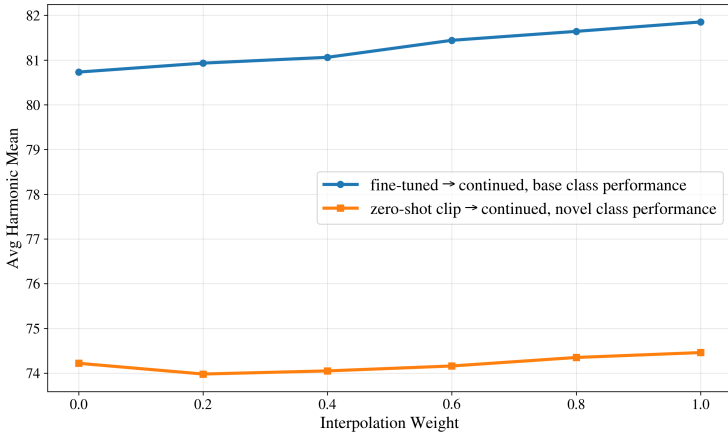


Figure 4: Linear mode connectivity analysis on base-to-novel generalisation. We interpolate between our continued model and both the zero-shot CLIP model (orange line, novel-class performance) and the fine-tuned KgCoOp model (blue line, base-class performance). The smooth paths confirm that MERGETUNE successfully establishes linear mode connectivity with both endpoints, maintaining strong performance throughout interpolation. Results are averaged over 11 datasets.

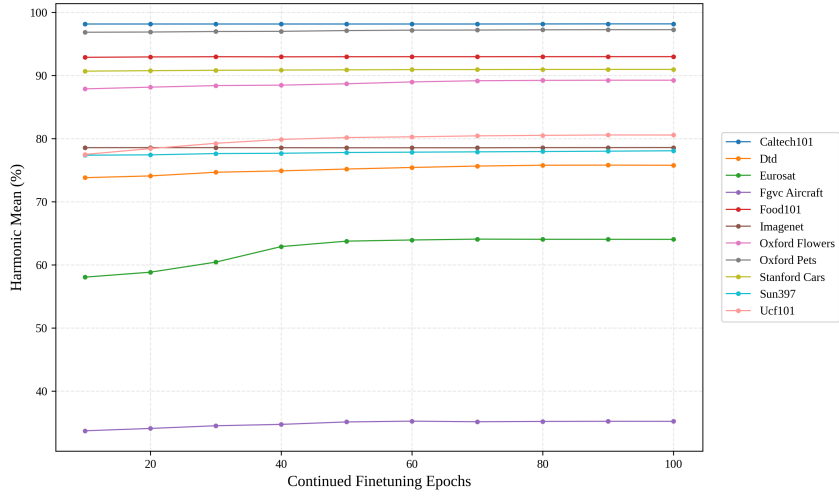


Figure 5: MERGETUNE exhibits no over-merging across extended training (ranging from 10 to 100 epochs). Performance trajectories across all 11 datasets show either stable performance or continuous improvement without degradation. No performance decline validates its robustness against over-merging through our dual-anchored linear mode connectivity objective.

line) shows stable, gradually improving base-class performance, while interpolation with zero-shot CLIP (orange line) maintains consistent, slightly improving novel-class performance throughout. The two smooth trajectories without performance fluctuations indicate that our continued model resides in a connected region of the loss landscape that spans both endpoints, confirming that MERGETUNE successfully establishes linear mode connectivity and effectively integrates knowledge from both the zero-shot and fine-tuned solutions.

A.3.5 WILL CONTINUED FINETUNING INTRODUCE OVER-MERGING?

To evaluate potential over-merging from our continued finetuning, we analysed MERGETUNE’s performance across all 11 datasets, ranging from 10 to 100 epochs using CoOp + MERGETUNE on Siglip2-B/16 (as in Figure 5). Results exhibit two primary patterns: stable performance (on Caltech101, Food101, Oxford Pets, and ImageNet) and continuous improvement (on DTD, Ox-

ford Flowers, Stanford Cars, UCF101, EuroSAT, and FGVC Aircraft). Across all datasets, no performance degradation is observed during continued finetuning, confirming that our linear-mode connectivity-guided model merging does not lead to over-merging, thanks to the effective regularisation applied to both zero-shot and fine-tuned endpoints.